Eur. Phys. J. B **17**, 103–109 (2000)

THE EUROPEAN PHYSICAL JOURNAL B

EDP Sciences
© Società Italiana di Fisica
Springer-Verlag 2000

Stabilization of A-type layered antiferromagnetic phase in $LaMnO_3$ by cooperative Jahn-Teller deformations

M. Capone[1], D. Feinberg[2,a], and M. Grilli[3]

[1] Istituto Nazionale di Fisica della Materia and International School for Advanced Studies (SISSA-ISAS), Via Beirut 2-4, 34013 Trieste, Italy
[2] Laboratoire d'Études des Propriétés Électroniques des Solides, CNRS, associated with Université Joseph Fourier, BP 166, 38042 Grenoble Cedex 9, France
[3] Istituto Nazionale di Fisica della Materia and Dipartimento di Fisica, Università di Roma "La Sapienza", Piazzale Aldo Moro 2, 00185 Roma, Italy

Received 24 January 2000

Abstract. It is shown that the layered antiferromagnetic order in stoechiometric $LaMnO_3$ cannot be understood purely from electronic interactions. On the contrary, it mainly results from strong cooperative Jahn-Teller deformation. Those involve a compression of the Mn–O octahedron along the c-axis (mode $Q_3 < 0$), while alternate Jahn-Teller deformations occur in the ab-plane (mode Q_2). These deformations stabilize a certain type of orbital ordering. The resulting superexchange couplings are calculated by exact diagonalization, taking into account both e_g and t_{2g} orbitals. The main result is that antiferromagnetic (ferromagnetic) coupling along the c-direction (ab-planes) can be understood only if the Jahn-Teller energy is much larger than the superexchange couplings, which is consistent with experiments. This mechanism contrasts with that based on weak Jahn-Teller coupling which instead predicts elongation along the c-axis ($Q_3 > 0$). The crucial role of the deformation anisotropy $\frac{Q_2}{Q_3}$ is also emphasized.

PACS. 71.70.Ej Spin-orbit coupling, Zeeman and Stark splitting, Jahn-Teller effect – 75.30.Et Exchange and superexchange interactions

1 Introduction

Perovskite oxides containing Mn ions have been the object of intense interest in the recent years. In spite of being known for a very long time, these compounds have been reconsidered in great detail owing to their colossal magnetoresistive properties. Starting from the "parent" phases $LaMnO_3$ (trivalent Mn) and $CaMnO_3$ (tetravalent Mn), substitutional doping has revealed an extremely rich phase diagram. Understanding this diagram requires at least the following ingredients: i) strong on-site Coulomb interactions; ii) the "double exchange" mechanism due to the interplay of e_g electron itineracy and Hund's exchange with the more localized t_{2g} electron spins, which favours ferromagnetism [1–3]; iii) superexchange between t_{2g} electrons as well as between e_g electrons on neighbouring sites; iv) large electron-lattice interactions, in particular due to Jahn-Teller (JT) effect on Mn^{3+} ions [4,5]. All these elements are necessary to understand the interplay between spin, charge and orbital ordering. The latter lifts the degeneracy of the e_g orbitals by a cooperative Jahn-Teller lattice deformation and leads to tetragonal or orthorhombic deformations of the cubic structure.

Although Goodenough [6] provided long time ago a qualitative understanding of the phase diagram of the $(La, Ca)MnO_3$ family, a full microscopic description is still lacking. Especially the dramatic dependence of all physical properties with very fine tuning of the chemical composition requires a precise estimate of the various parameters, and clear identification of the dominant mechanism for every doping. Surprisingly enough, such an understanding is not yet reached in the insulating antiferromagnet $LaMnO_3$, although it seems essential before quantitatively studying the doped phases. This phase, when fully stoechiometric, presents a layered antiferromagnetic order, with ferromagnetic couplings (F) in two directions and antiferromagnetic (AF) coupling in the other [7]. The AF directions are associated to a shortening of the Mn–O bonds, leading to tetragonal distortion, while in the F directions long and short bonds alternate, yielding the overall orthorhombic structure. In what follows, we shall neglect the tilting of the Mn–O octahedra and concentrate only on the Mn–O bond length deformations. These can be understood in terms of cooperative JT effect. The corresponding lifting of e_g degeneracy can be viewed as an orbital ordering, with occupied d orbitals pointing preferentially in the directions of long Mn–O bonds.

[a] e-mail: feinberg@lepes.polycnrs-gre.fr

Several proposals have been made to explain layered antiferromagnetism in $LaMnO_3$. Goodenough [6] used the picture of "semi-covalence" where oxygen orbitals play an essential role in overlapping empty d orbitals of Mn ions. This picture, although useful for qualitative purposes, has not received confirmation by microscopic calculations and does not allow to write simple enough models, for instance based on a Hamiltonian involving only metal orbital electrons and their basic interactions. A microscopic description requires to identify clearly the dominant interactions in the problem. In pioneering works, Kugel and Khomskii [8], and Lacroix [9] (see also earlier work by Roth [10]), proposed that superexchange in the presence of e_g orbital degeneracy results in ferromagnetism and orbital ordering: Hund's rule favours in this case different orbitals on neighbouring sites and ferromagnetic coupling. Using a simplified model with equal hopping integrals between e_g orbitals leads to the same ordering along the three cubic lattice directions: the resulting structure is an insulating ferromagnet, with "antiferroorbital" ordering. However, taking properly into account the hopping integrals between $d_{x^2-y^2}$ (denoted x) and d_{z^2} (denoted z) orbitals, Kugel and Khomskii [8] found the correct magnetic structure. Starting with degenerate e_g orbitals, they performed a perturbative calculation in $\frac{t}{U}$ and $\frac{J_{\rm H}}{U}$ where t, $J_{\rm H}$ and U are the typical hopping integral, the Hund coupling and the on-site repulsion in the order. Based on the weak electron-lattice coupling in the compound $KCuF_3$, they considered the JT couplings as a perturbation. As a result, orbital and magnetic ordering result from superexchange (SE) only: Intraorbital SE dominates in the c-direction (defined as the z-axis), leading to AF coupling, while interorbital SE dominates in the ab-directions, yielding F coupling. Occupied orbitals are dominantly $d_{z^2-x^2}$ and $d_{z^2-y^2}$, therefore, as Kugel and Khomskii remark, for Cu^{2+} in $KCuF_3$ (hole orbital), JT coupling implies a shortening as experimentally observed ($c/a < 1$). However, for Mn^{3+} ions with one electron in the e_g levels, they correctly point out that repulsion between metal and anion orbitals, together with JT coupling, would trigger a lengthening of the c-axis ($c/a > 1$), in contradiction with the actual structure. In a recent work, Feiner and Oles [11] reconsidered Kugel and Khomskii's model, including both Hund's coupling between e_g and t_{2g} orbitals and the antiferromagnetic superexchange interaction between t_{2g} spins (equal to $\frac{3}{2}$ in the ground state). Their results confirms those of reference [8]: They find the correct layered structure (which they call MOFFA), but only if the d_{z^2} orbital has lower energy than the $d_{x^2-y^2}$ one, contrarily to what happens for electron-like orbitals (case of $LaMnO_3$). This contradiction sets the limits of the Kugel-Khomskii model for $LaMnO_3$. We believe that the JT effect, on the contrary, has to be considered from the very beginning in the model.

Essentially, the assumption that the e_g degeneracy is lifted principally by superexchange may be justified in $KCuF_3$, but is definitely not correct in $LaMnO_3$. In fact, this could hold only if the typical JT splitting ϵ was much smaller than the superexchange splitting, of order $\frac{t^2}{U}$. The latter (related to the magnetic transition temperatures) being of the order of a few meV, the former is much larger. Although there is no precise evaluation of this quantity, this is supported by experiment: On the one hand, the deformations of Mn–O bonds is extremely large, more than ten per cent, indicating that $\epsilon > k_{\rm B}T$. On the other hand, neutron scattering measurements show that the local distorsions persist above the orthorhombic-cubic transition at 750 K [12]. This temperature only marks the disappearance of cooperative JT ordering, while distorted MnO_6 octahedra still exist at higher temperatures. Photoemission [13] measurements indicate that JT splittings are as large as a few tenth of eV, comparable to the electronic hopping integrals between neighbouring sites. And optical conductivity analysis [14] also shows evidence of large splittings.

In these conditions, the degenerate perturbation calculation of reference [8] does not hold anymore. In a previous work we have reconsidered the problem within perturbation theory [15], making the opposite assumption, *i.e.* $\epsilon \gg \frac{t^2}{U}$: This means that, given the crystal deformations, due to strong cooperative JT effect, the e_g orbitals split so as to give a certain type of orbital ordering. The orbitals stabilized at each sites are different from the one predicted by pure superexchange. We have found that, depending on the values of the two JT modes Q_2 and Q_3, different magnetic ordering could be stabilized, among which the layered "FFA". This ordering is always stabilized if the Q_3 mode is positive, *e.g.* for dilatation in the c-direction. But in the real case $Q_3 < 0$, FFA order is realized only if the in-plane alternate Q_2 mode is sufficiently large and overcomes the contrary effect of Q_3. Looking at structural numbers, one checks that this is actually the case. Nevertheless the system is close to the point where the FFA order becomes unstable towards FFF. This results in the F exchange (along the ab-plane) being larger than the AF exchange (along the c-axis). This feature has been obtained from inelastic neutron scattering [16], and it cannot be explained by the Kugel-Khomskii model, which obtains on the contrary that the F superexchange is of order $\frac{J_{\rm H}}{U}$ times the AF one, thus much smaller.

The interplay between lattice distortions and magnetism has also been investigated from *ab initio* calculations of the electronic structures [17–19]. All conclude with a prominent role of those distortions to stabilize the actual magnetic order. In particular, Solovyev *et al.* [18] have found that the c-axis exchange is antiferromagnetic only if the JT distortion is sufficiently large. For $LaMnO_3$ with its very large distortion they obtain the layered antiferromagnetic structure, but it is close to the border between FFA and FFF phases. Very recent Monte Carlo calculations have also demonstrated the relevance of the JT interaction in stabilizing the FFA magnetic order [20].

In the present work, we reconsider the problem, beyond any perturbation theory, by exact diagonalizations on pairs of Mn^{3+} sites. The two e_g orbitals are considered together with the quantum $\frac{3}{2}$-spins due to the electrons in the t_{2g} levels. Our conclusions confirm the essential role of JT deformations, especially the Q_2 mode, to stabilize

the layered AF order. They also demonstrate that it is essential to include Hund's coupling with t_{2g} orbitals, and that the role of the intrinsic t_{2g} AF exchange is to slightly stabilize the FFA order with respect to the FFF one.

2 The model

From the discussion of the preceding section it is clear that the basic physical ingredients required for a satisfactory description of the manganites should involve both Coulomb and lattice (namely JT) interactions. Accordingly we consider the following model

$$H = H_t + H_{\rm H} + H_{UU'} + H_{\rm J} + H_{\rm JT} \tag{1}$$

with

$$\begin{aligned}
H_{\rm t} &= -\sum_{i\mathbf{a}\alpha\alpha'\sigma} t^{\mathbf{a}}_{\alpha\alpha'} c^\dagger_{i\alpha\sigma} c_{i+\mathbf{a}\alpha'\sigma} \\
H_{\rm H} &= -J_{\rm H} \sum_{i\alpha\sigma\sigma'} c^\dagger_{i\alpha\sigma} \mathbf{s}_{\sigma\sigma'} c_{i\alpha\sigma'} \\
&\quad \times \left[\mathbf{S}_i + \sum_{\alpha'\neq\alpha\tilde{\sigma}\tilde{\sigma}'} c_{i\alpha'\tilde{\sigma}} \mathbf{s}_{\tilde{\sigma}\tilde{\sigma}'} c_{i\alpha'\tilde{\sigma}'} \right] \\
H_{UU'} &= U \sum_{i\alpha} \left(c^\dagger_{i\alpha\uparrow} c_{i\alpha\uparrow} \right) \left(c^\dagger_{i\alpha\downarrow} c_{i\alpha\downarrow} \right) \\
&\quad + U' \sum_{i\alpha\neq\alpha'\sigma\sigma'} \left(c^\dagger_{i\alpha\sigma} c_{i\alpha\sigma} \right) \left(c^\dagger_{i\alpha'\sigma'} c_{i\alpha'\sigma'} \right) \\
H_{\rm J} &= J_t \sum_{\langle ij \rangle} \mathbf{S}_i \cdot \mathbf{S}_j \\
H_{\rm JT} &= g \sum_i \Big(c^\dagger_{i\alpha\sigma} \tau^{(\mathbf{3})}_{\alpha\alpha'} c_{i\alpha'\sigma} Q_{3i} + c^\dagger_{i\alpha\sigma} \tau^{(\mathbf{2})}_{\alpha\alpha'} c_{i\alpha'\sigma} Q_{2i} \Big).
\end{aligned}$$

The first term represents the kinetic energy with the electrons in the manganese $3d_{x^2-y^2}$ ($\alpha = x$) or $3d_{3z^2-r^2}$ ($\alpha = z$) orbitals hopping from site i to the nearest neighbor (nn) site $i + \mathbf{a}$ in the $\mathbf{a}$ lattice direction. Here $\mathbf{s}$ is the vector of Pauli matrices for spins and τ the vector of Pauli matrices for orbital pseudospins in the x, z basis. Specifically, for a standard choice of the phases for the orbital wavefunctions, the hopping between the x and the z orbitals are given by

$$\begin{aligned}
&t^{\mathbf{x},\mathbf{y}}_{xx} = 3t; \quad t^{\mathbf{x},\mathbf{y}}_{zz} = -t; \\
&t^{\mathbf{x}}_{xz} = -\sqrt{3}t; \quad t^{\mathbf{y}}_{xz} = \sqrt{3}t \\
&t^{\mathbf{z}}_{zz} = -4t \quad t^{\mathbf{z}}_{xx} = t^{\mathbf{z}}_{xz} = 0\,.
\end{aligned} \tag{2}$$

Together with the Hund coupling given by $H_{\rm H}$ the kinetic energy gives rise to the usual "double-exchange" itinerancy of the e_g electrons. The (strong) on-site Coulomb interactions, are represented by the intraorbital repulsion U and by the interorbital $U' = U - 2J_{\rm H}$ term.

For simplicity here and in the following we will not distinguish between the Hund exchange energy between electrons in the e_g and t_{2g} orbitals. The antiferromagnetic superexchange coupling between neighboring t_{2g} spins is considered with $H_{\rm J}$, while the JT interaction between the e_g electrons and the (cooperative) lattice deformation is given by the last term $H_{\rm JT}$. The Jahn-Teller modes are defined in terms of the short (s), medium (m) and long (l) Mn–O bonds by $Q_2 = \sqrt{2}(l-s)$ and $Q_3 = \sqrt{2/3}(2m - l - s)$, the m bonds lying in the z direction and the s, l ones in the x, y planes. With this convention, both $KCuF_3$ and $LaMnO_3$ show compression along the c-axis, *e.g.* $Q_3 < 0$. On the other hand, due to the respectively hole-like and electron-like character of the relevant e_g orbital states, the coupling constant g is negative in $KCuF_3$, and positive in $LaMnO_3$ where the $d_{x^2-y^2}$ orbital is favoured ($\tau_z = +1$). In what follows, we redefine Q_3 as Q_3 sgn(g), *e.g.* $Q_3 > 0$ in $KCuF_3$ and $Q_3 < 0$ in $LaMnO_3$.

Since in the present work we will not attempt to perform any energy minimization by including the elastic interactions due to the lattice, we here disregard these energy terms by treating the JT deformations $\mathbf{Q} = (Q_2, Q_3)$ as external fields imposed by a lattice ordering involving a much higher energy scale than the magnetic ones. Therefore in the following the various magnetic couplings will be determined in terms of *assigned* lattice deformations. This viewpoint, which already guided us in the perturbative analysis of the stability of FFA antiferromagnetism in the undoped LMO [15] is definitely justified by the experimental observation that the JT energy splitting is much larger than all magnetic couplings.

We exactly diagonalize the Hamiltonian in equation (1) for a system of two sites with open boundary conditions. The two sites are located either on the same xy plane or on adjacent planes and the suitable hopping matrix elements between the various orbitals have been considered according to expressions (2).

The JT energy splitting $\epsilon = g\sqrt{Q_2^2 + Q_3^2}$ and the deformation anisotropy ratio $r \equiv Q_2/Q_3$ are given external parameters and are fixed for any diagonalization procedure. Once the ground state is found, the effective exchange coupling between the total spins on the two sites can be determined. Specifically, since the Hamiltonian conserves the total spin of the two-site cluster, we determine the ground states with total spin $S_{\rm T} = 4, M_{S_{\rm T}} = 4$ and $S_{\rm T} = 3, M_{S_{\rm T}} = 3$. Then the magnetic coupling is given by the energy difference $E(S_{\rm T} = 4, M_{S_{\rm T}} = 4) - E(S_{\rm T} = 3, M_{S_{\rm T}} = 3) = 2J$. Once the magnetic couplings (and particularly their sign) along the various lattice directions are found, the resulting magnetic phase is also determined.

3 Results

In order to gain insight from the physical processes underlying the intersite magnetic couplings, we first carry out a comparison between the results of the perturbative analysis of the superexchange interactions (see Ref. [15]) and the exact numerical calculations. The perturbative analysis not only was performed assuming very large local Coulomb interactions (U, U' and $J_{\rm H}$ much larger than t), but the additional assumption was made that the JT energy splitting ϵ greatly exceeds the typical superexchange

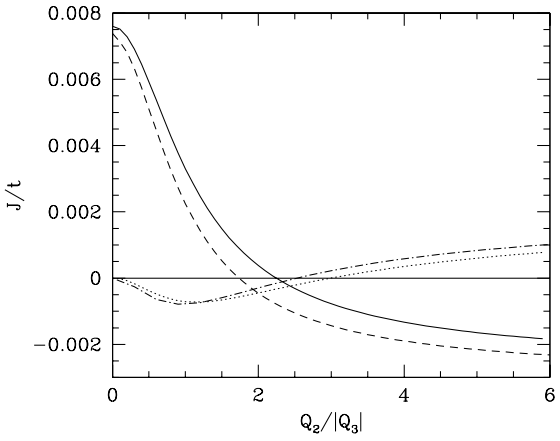

Fig. 1. Magnetic couplings for $Q_3 < 0$, $t = 0.2$ eV, $U = 8$ eV, $J_{\rm H} = 1.2$ eV, $\epsilon = 0.4$ eV, and $J_t = 0$ as function of the deformation anisotropy ratio from exact diagonalization and perturbation theory. Dashed line: J_{xy} from exact diagonalization; dot-dashed line: J_z from exact diagonalization; solid line: J_{xy} from perturbation theory; dotted line: J_z from perturbation theory. Negative (resp. positive) values indicate ferro (resp. antiferro) magnetic interactions.

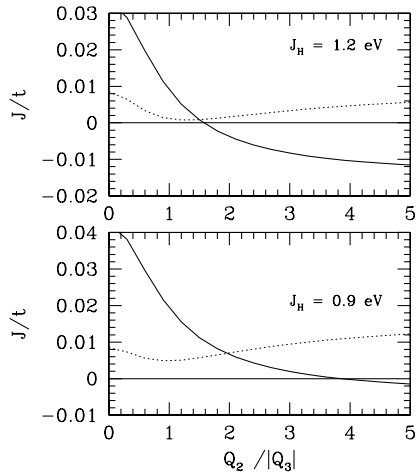

Fig. 2. Magnetic couplings J_{xy} (solid line) and J_z (dotted line) *vs.* the deformation ratio $r = Q_2/|Q_3|$ for negative values of Q_3, for $t = 0.14$ eV, $U = 6$ eV, $\epsilon = 0.3$ eV, $J_t = 2.1$ meV and $J_{\rm H} = 1.2$ eV ($J_{\rm H} = 0.9$ eV) in the upper (lower) panel.

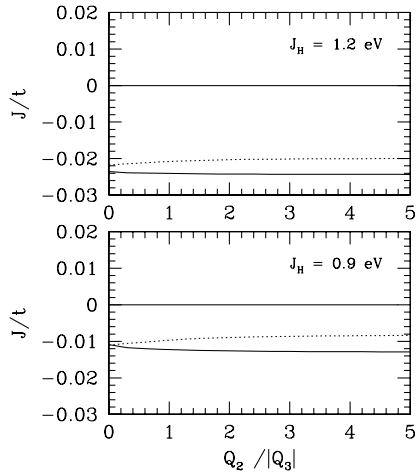

Fig. 3. Magnetic couplings (see Fig. 2) *vs.* the deformation ratio $r = Q_2/|Q_3|$ for negative values of Q_3, for $t = 0.14$ eV, $U = 6$ eV, $\epsilon = 0.01$ eV, $J_t = 2.1$ meV and $J_{\rm H} = 1.2$ eV ($J_{\rm H} = 0.9$ eV) in the upper (lower) panel.

energy scale of order t^2/U. In this way the ground state can safely be assumed to be formed by just one singly occupied e_g level. Accordingly the exact numerical calculations to be compared with the analytic results have been performed for $Q_3 < 0$ and $t = 0.2$ eV, $U = 8$ eV, $J_{\rm H} = 1.2$ eV, $\epsilon = 0.4$ eV, and $J_t = 0$. Figure 1 reports the superexchange interactions both in the planar and interplanar directions obtained with both the perturbative and the exact-diagonalization analysis. As it is apparent, the perturbative J_{xy} and J_z display the same qualitative behavior as in the exact calculation. This confirms that, at least in the $\epsilon \gg t^2/U$ limit, a substantial part of the magnetic effective interactions is generated by the superexchange processes due to the hopping of electrons lying in the lower e_g level on the same or on different nearest neighbor e_g orbitals. On the other hand, the quantitative comparison indicates that the range of stability for the FFA phase (*i.e.* $J_{xy} < 0$ and $J_z > 0$) is modified. In fact a positive J_z together with a negative J_{xy} are obtained in the exact calculation on a somewhat larger range of lattice deformation anisotropies ($Q_2/|Q_3| \geq 2.5$). In order to establish a tighter connection between the experimentally determined J's and the observed deformations, and to investigate the role of the various interactions in the model, a more systematic analysis is required. Assuming the JT interaction to be relevant in stabilizing the FFA phase, we investigate the behavior of the exchange constants J_{xy} (denoted "intraplane") and J_z (denoted "interplane") in terms of ϵ and the deformation ratio r.

Figures 2 and 3 report J_{xy} and J_z as functions of $|r|$ for the $Q_3 < 0$ case (the one relevant for LMO) at a large ($\epsilon \sim 2t$) and at a small ($\epsilon < 0.1t$) value of the JT splitting respectively. Different values of the Hund coupling $J_{\rm H}$ are considered. One can first observe from Figure 2 that in the large-ϵ case the increase of the Hund coupling shifts downwards both the intraplane and the interplane magnetic couplings. This outcome can be rationalized in terms of perturbatively generated superexchange processes providing AF effective couplings of the form

$$J^{\rm AF}_{xy,z} \approx \frac{A_{xy,z}}{U + (3/2)J_{\rm H}} + \frac{B_{xy,z}}{U + \epsilon} \qquad (3)$$

competing with the generated F interaction

$$J^{\rm F}_{xy,z} \approx -\frac{C_{xy,z}}{U + \epsilon - (5/2)J_{\rm H}} \,. \qquad (4)$$

The numerical coefficients A, B, and C stem from the different hopping matrix elements between the different orbitals in the different directions [15]. Specifically, while the A's are related to the hopping processes between two nearest-neighbour lower-lying e_g orbitals, the B and C coefficients are due to hoppings between one low-lying and

one higher JT-split orbitals (this is why the corresponding denominators involve ϵ). The A, B and C coefficients are independent of the Coulomb interactions, which only determine the energies of the virtual intermediate states in the superexchange processes. The above schematic expressions clearly show that, when $J_{\rm H}$ is increased for a fixed $\epsilon \gg t$, the F spin configuration becomes more favourable, since the F coupling become stronger, while the AF interaction weakens. We remark that purely electronic models such as in references [8,11] make use of degenerate perturbation theory. Then the orbital splitting is of order of the exchange couplings J and therefore those models become invalid if $\epsilon > J$, which is the case in $LaMnO_3$. More seriously, the orbital order resulting from purely electronic interactions is at odds with that obtained from the actual Jahn-Teller distortions, showing that those distortions do not result from an orbital ordering of electronic origin, but are on the contrary the mere source of orbital ordering.

Another quite generic effect, which can be interpreted in terms of perturbatively generated superexchange processes is the tendency of J_z to acquire a F (or at least a less AF) character at low values of $Q_2/|Q_3|$ (this can also be accompanied by an upturn of J_z for $|r|$ tending to zero). This occurs because for $Q_3 < 0$, the lowest e_g level progressively loses its $3d_{3z^2-r^2}$ component: By schematically writing the lower and the upper e_g states as $|a\rangle \propto |x\rangle + \eta|z\rangle$ and $|b\rangle \propto -\eta|x\rangle + |z\rangle$ respectively, η vanishes with $|r| \to 0$. Now, the superexchange along z is driven by the interplane hopping, which is only allowed between $3d_{3z^2-r^2}$ orbitals. Furthermore one can see [15] that the ferromagnetic superexchange arises from $|a\rangle \to |b\rangle$ hoppings, which are of order η, while the antiferromagnetic coupling is mostly generated from intraorbital $|a\rangle \to |a\rangle$ hopping (the A term in Eq. (3)). Since this latter is of order η^2, it is quite natural that in the low-$|r|$ region, as η decreases, the superexchange along z is ferromagnetic and vanishes with η. This ferromagnetic tendency is, however, contrasted (and actually overcome in Figs. 2 and 3) by the independent AF superexchange J_t between the t_{2g} spins, which becomes relatively more important. Of course, when $|r|$ increases, the η^2 terms in the hopping become relevant, the intraorbital $|a\rangle \to |a\rangle$ hopping starts to dominate and J_z eventually becomes (more) positive (*i.e.* AF).

As far as the superexchange along the planes is concerned, at small $|r|$ this is instead dominated by the large hopping between $3d_{x^2-y^2}$ orbitals, which favor the $|a\rangle \to |a\rangle$ hopping and, consequently produces an AF magnetic coupling. On the contrary, for large $|r|$, orbital ordering implies that the main superexchange contribution comes from hopping between different orbitals, thus favouring ferromagnetism [8].

All the above arguments are obviously only valid as long as the conditions for the perturbation theory nearly hold. On the other hand, the simple perturbative approach between non-degenerate states breaks down when $\epsilon \approx t^2/U$ as in Figure 3 and the interpretation of the results is not so transparent. However, the effect of $J_{\rm H}$ favoring ferromagnetism is still present.

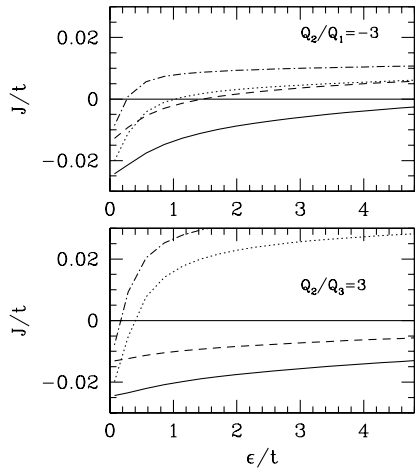

Fig. 4. Magnetic couplings *vs.* the JT splitting energy ϵ for $t = 0.14$ eV, $U = 6$ eV, $J_t = 2.1$ meV for $Q_2/Q_3 = -3$ (upper panel) and $Q_2/Q_3 = 3$ (lower panel). Solid line: J_{xy} for $J_{\rm H} = 1.2$ eV; dotted line: J_z for $J_{\rm H} = 1.2$ eV; dashed line: J_{xy} for $J_{\rm H} = 0.9$ eV; dot-dashed line: J_{xy} for $J_{\rm H} = 0.9$ eV.

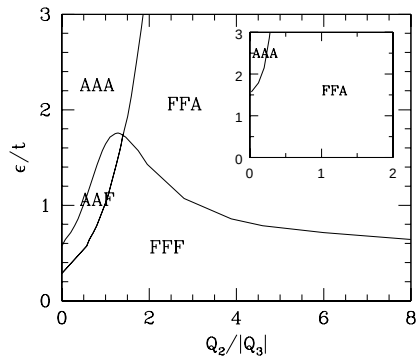

Fig. 5. Zero-temperature phase diagram for $t = 0.14$ eV, $U = 6$ eV, $J_t = 2.1$ meV and $J_{\rm H} = 1.2$ eV.

An important difference between the results in Figures 2 and 3 is that the FFA phase is generically obtained in a broad range of parameters when $\epsilon \gg t$. In particular, for rather realistic values of $J_{\rm H} \sim 5t \approx 1$ eV the deformation ratios required to generate negative (*i.e.* F) couplings in the xy planes and positive ones in the z direction are quite reasonable $|r| \sim 2$–3. The same does not hold in the case of small JT splitting, where J_{xy} and J_z have the same sign (FFF). Therefore a first result is that a sizable ϵ is needed in order to obtain both the FFA phase and reasonable lattice distortion ratios Q_2/Q_3.

This result is also confirmed by the calculation of J_{xy} and J_z as a function of ϵ, at a fixed value of the deformation anisotropy ratio r. Figures 4 and 5 report the values of J_{xy} and J_z for $r = 3$ and $r = -3$ respectively. While the positive r case is generic for perovskite materials with the lattice elongated in the z direction ($c/a > 1$), the latter choice is more pertinent to the case of the undoped LMO, where $c/a < 1$. As already discussed by Kugel and Khomskii [8] for a different model and as confirmed by the perturbative analysis of reference [15], the JT deformation and the superexchange interactions cooperate when

$Q_3 > 0$ like in $KCuF_3$ so that it is not surprising that for all values of J_H the FFA is realized over a much broader range of ϵ. On the other hand, for $Q_3 < 0$, Figure 4 shows that the conditions for a FFA phase, $J_{xy} < 0$ and $J_z > 0$, are only realized for a smaller range of ϵ values. In particular a sizeable minimum value of ϵ is required to have an AF coupling along z, while exceedingly large values of ϵ (of order $J_{\rm H}$) produce an AF coupling also along the planes. Both the minimum and the maximum values of ϵ for obtaining the FFA phase increase upon increasing $J_{\rm H}$. However, the maximum value of ϵ increases more rapidly and the overall effect is that, increasing $J_{\rm H}$, the available range in ϵ to obtain an FFA phase is enlarged. Again the behavior displayed in the exact calculations reported in Figure 4 can easily be interpreted in terms of the perturbative superexchange processes schematically represented in equations (3, 4). First of all these expressions at once account for the increasing behavior of the couplings upon increasing ϵ: While only the interorbital part of $J_{\rm AF}$ (the contribution proportional to B) decreases upon increasing ϵ, the whole ferromagnetic part in equation (4) is suppressed when ϵ grows, so that the total coupling, although ferromagnetic at small JT energy splitting, eventually vanishes and becomes positive.

Moreover it turns out that, for $|r| > 2 - 3$ the hoppings generate smaller A, B, C coefficients in the z direction. This accounts for the more rapid rise of J_z when ϵ is increased. Finally, along the same line of the discussion of Figure 2, one can easily observe that an increasing $J_{\rm H}$ strengthens the ferromagnetic component and weakens the antiferromagnetic one, thus rationalizing the generic tendency of all curves to be shifted downwards when $J_{\rm H}$ grows.

Besides the above specific findings, the occurrence of the various magnetic phases can be cast in a phase diagram at zero temperature illustrating the stability region of these phases in terms of the JT energy splitting and the deformation ratio. In the light of their richer complexity and of the present interest in the Manganites, we here consider in greater detail the case of $Q_3 < 0$ of relevance for the undoped LMO, while the $Q_3 > 0$ case is only described in the inset of Figure 5. Figures 5 and 6 report the phase diagram for two different values of the Hund coupling. Both phase diagrams display the same qualitative features. In particular, at moderate and large values of ϵ a Néel AAA phase is found for weak planar distortions (small r). As seen in the discussion of Figure 2, in the very-small-r region, J_{xy} is naturally positive, while the superexchange between e_g levels along z, although ferromagnetic, is small so that the direct superexchange between t_{2g} spins may easily dominate and gives rise to the AAA phase (see Figs. 2 and 3). As it can be also be seen from Figure 1, it can be checked that the AAA phase is replaced by the so-called C-like antiferromagnetic AAF phase in the $J_t = 0$ case. At small-to-intermediate values of ϵ, a progressive increase of $|r|$ drives the system towards the phase AAF. In this phase J_{xy} keeps its AF character, while the negative superexchange between e_g levels along z is small, but no longer is overcome by J_t. At larger values of ϵ the AAF phase is not present, but the intimate nature of the AAA phase changes upon increasing $|r|$. In particular while at low $|r|$ the AF along z is determined by J_t, at larger $|r|$, the superexchange between e_g levels along z is itself AF and therefore the t_{2g} superexchange contributes, but it is not strictly necessary to the AF coupling along z. On the other hand, a further increase of $|r|$ promotes a F coupling along the planes and leads to the A-type antiferromagnetism FFA experimentally observed in undoped LMO.

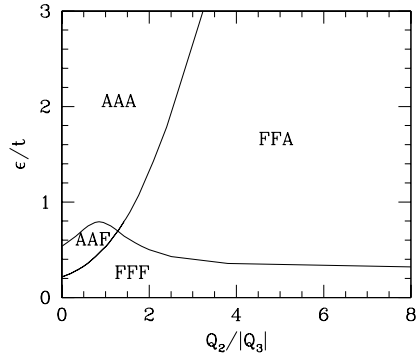

Fig. 6. Zero-temperature phase diagram for $t = 0.14$ eV, $U = 6$ eV, $J_t = 2.1$ meV and $J_{\rm H} = 1.0$ eV.

At small values of the JT splitting, the phase diagram is prominently occupied by a FFF phase. In this latter regard, from the comparison of Figures 5 and 6, the important observation can be done that the FFF phase at low and moderate ϵ's is greatly stabilized by the increase of the Hund coupling J_H, as previously expected.

Within the present exact numerical treatment of the model in equation (1) it is also possible to attempt at "precise" estimates of J_{xy} and of J_z. As an example, we report here a realistic sets of parameters (among many others) providing the values $J_{xy} = -0.83$ meV and $J_z = 0.58$ meV experimentally observed with inelastic neutron scattering [16]. Assuming $Q_2/|Q_3| = 3.2$, a value largely confirmed by many groups [12], we take $t = 0.124$ eV, $U = 5.81$ eV, $J_{\rm H} = 1.2$ eV, $J_t = 2.1$ meV, and $\epsilon = 0.325$ eV. The quite reasonable values of the model parameters needed to reproduce the measured magnetic couplings is an indirect test of the validity of the considered model. We emphasize that the "anomalous" trend $|J_{xy}| > |J_z|$ is correctly reproduced, and that our fit is relatively flexible concerning parameters U, $J_{\rm H}$ or t, provided ϵ is large enough.

4 Conclusions

In this paper we presented the results of calculations based on the exact diagonalization of a model aiming to describe the stoechiometric $LaMnO_3$. The model includes strong local Coulomb interactions as well as a JT coupling between the electrons and the Q_2 and Q_3 lattice deformations.

Despite the smallness of our cluster, we believe that our determination of the magnetic couplings not only

is qualitatively, but also quantitatively significant. This is so because, in the presently considered undoped LMO, the coherent charge mobility is negligible due to the large on-site Coulomb repulsions and to the substantial JT deformations. As a consequence the magnetic interactions do not arise, *e.g.*, from Fermi surface instabilities or other collective effects, but are rather determined by short-distance (incoherent) processes.

One first relevant result is that, when the Mn–O octahedron is compressed along z, a FFA phase is only obtained for a sizable (staggered) Q_2 deformation of the planar unit cell. This finding agrees with the *ab initio* calculations of reference [18].

Our analysis also points out the relevant role played by the Hund coupling, which generically emphasizes the ferromagnetic component of the superexchange processes. Quite relevant turns out to be also the Hund coupling between the e_g electrons and the t_{2g} spins. In this latter regard, we explicitly checked that, keeping $J_{\rm H}$ finite between the e_g electrons, but decoupling them from the t_{2g} spins no longer gives rise to the FFF phase at low values of the JT splitting (*cf.* the phase diagrams in Figs. 6 and 7). Instead at $\epsilon \sim 0$ a FFA phase is found in agreement with the results of reference [8] for a model, which only considered e_g electrons and no JT splitting. This indicates that the determination of the stable phase (at least) at small values of the JT energy must take in due account the Hund coupling thereby including the t_{2g} levels. Secondly a quantitative determination of the stability region for the FFA phase and of the value of the magnetic couplings is subordinate to the consideration of the $J_{\rm H}$ term.

Our work shares with reference [20] the generic result that JT distortions strongly affect the magnetic structure. Nevertheless it is worth pointing out some differences. In a certain respect our work is less ambitious in so far it does not attempt to determine the JT distortions, but it rather imposes them as external parameters of the calculation. Actually we do not believe that such deformations can be easily determined by microscopic models, which should incorporate complex effects such as long-range Coulomb interactions, cation and anion size and tilts of the MnO_6 octahedra. On the other hand realistic deformations as obtained from experiments can easily be imposed and the consequent local electronic structure can be determined exactly: orbital ordering results essentially from cooperative Jahn-Teller deformations.

Moreover, and quite importantly for a quantitative determination of the magnetic coupling and of the stability of the magnetic phases, we here also take into account the electronic Coulomb repulsion. This interaction is perforce larger than the JT interaction and contributes to its insulating behavior as well as to the numerical values of the exchange couplings.

Finally we showed that using reasonable parameters the experimental values of the magnetic couplings can easily be reproduced. Of course precise estimates depend on the knowledge of the various couplings entering the model, which are not always available neither from experiments nor from reliable first principle calculations. However calculating the magnetic couplings for various parameters and matching the numerical results with the experimentally obtained values provides useful connections between the involved parameters and set limits to the poorly known physical quantities.

References

1. C. Zener, Phys. Rev. **82**, 403 (1951).
2. P.W. Anderson, H. Hasegawa, Phys. Rev. **100**, 675 (1955).
3. P.G. de Gennes, Phys. Rev. **118**, 141 (1960).
4. A.J. Millis, P.B. Littlewood, B.I. Shraiman, Phys. Rev. Lett. **74**, 5144 (1995).
5. J. Zang, A.R. Bishop, H. Röder, Phys. Rev. B **53**, 8840 (1996).
6. J.B. Goodenough, Phys. Rev. **100**, 564 (1955).
7. E.O. Wollan, W.C. Koehler, Phys. Rev. **100**, 545 (1955).
8. K.I. Kugel', D.I. Khomskii, Sov. Phys. JETP **37**, 725 (1973) (Zh. Eksp. Teor. Fiz. **64**, 1429 (1973)).
9. C. Lacroix, J. Phys. C **13**, 5125 (1980); C. Lacroix, Ph.D. thesis, Université de Grenoble, 1979 (in French).
10. L.M. Roth, Phys. Rev. **149**, 306 (1966).
11. L.F. Feiner, A.M. Oleś, Phys. Rev. B **59**, 3295 (1999).
12. J. Rodríguez-Carjaval, M. Hennion, F. Moussa, H. Moudden, L. Pinsard, A. Revcolevschi, Phys. Rev. B **57**, 3189 (1998).
13. D.S. Dessau, Z.-X. Shen, in *Colossal Magnetoresistance Oxides*, edited by Y. Tokura (Gordon & Breach, Monographs in Cond. Matt. Science, 1999).
14. J.H. Jung, K.H. Kim, D.J. Eom, T.W. Noh, E.J. Choi, J. Yu, Y.S. Kwon, Y. Chung, Phys. Rev. B **55**, 15489 (1997).
15. D. Feinberg, P. Germain, M. Grilli, G. Seibold, Phys. Rev. B **57**, 5583 (1998).
16. F. Moussa, M. Hennion, J. Rodríguez-Carjaval, H. Moudden, L. Pinsard, A. Revcolevschi, Phys. Rev. B **54**, 15149 (1996).
17. W.E. Pickett, D.J. Singh, Phys. Rev. B **53**, 1146 (1996).
18. I. Solovyev, N. Hamada, K. Terakura, Phys. Rev. Lett. **76**, 4825 (1996).
19. H. Sawada, Y. Morikawa, K. Terakura, N. Hamada, Phys. Rev. B **56**, 12154 (1997).
20. T. Hotta, S. Yunoki, M. Mayr, E. Dagotto, Phys. Rev. B **60**, 15009 (1999).